BIOCHEMISTRY
including biophysical chemistry & molecular biology

Article

pubs.acs.org/biochemistry

Mechanism and Diversity of the Erythromycin Esterase Family of Enzymes

Mariya Morar, Kate Pengelly, Kalinka Koteva, and Gerard D. Wright*

M. G. DeGroote Institute for Infectious Disease Research, Department of Biochemistry and Biomedical Sciences, McMaster University, Hamilton, Ontario L8N 3Z5, Canada

Supporting Information

ABSTRACT: Macrolide antibiotics such as azithromycin and erythromycin are mainstays of modern antibacterial chemotherapy, and like all antibiotics, they are vulnerable to resistance. One mechanism of macrolide resistance is via drug inactivation: enzymatic hydrolysis of the macrolactone ring catalyzed by erythromycin esterases, EreA and EreB. A genomic enzymology approach was taken to gain insight into the catalytic mechanisms and origins of Ere enzymes. Our analysis reveals that erythromycin esterases comprise a separate group in the hydrolase superfamily, which includes homologues of uncharacterized function found on the chromosome of *Bacillus cereus*, Bcr135 and Bcr136, whose three-dimensional structures have been determined. Biochemical characterization of Bcr136 confirms that it is an esterase that is, however, unable to inactivate macrolides. Using steady-state kinetics, homology-based structure modeling, site-directed mutagenesis, solvent isotope effect studies, pH, and inhibitor profiling performed in various combinations for EreA, EreB, and Bcr136 enzymes, we identified the active site and gained insight into some catalytic features of this novel enzyme superfamily. We rule out the possibility of a Ser/Thr nucleophile and show that one histidine, H46 (EreB numbering), is essential for catalytic function. This residue is proposed to serve as a general base in activation of a water molecule as the reaction nucleophile. Furthermore, we show that EreA, EreB, and Bcr136 are distinct, with only EreA inhibited by chelating agents and hypothesized to contain a noncatalytic metal. Detailed characterization of these esterases allows for a direct comparison of the resistance determinants, EreA and EreB, with their prototype, Bcr136, and for the discussion of their potential connections.

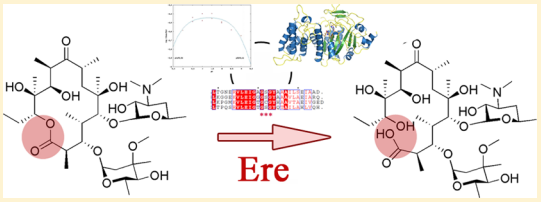

Macrolide natural products and their semisynthetic derivatives are important clinically relevant agents used to treat infectious disease. These drugs were first introduced into the clinic in 1952 as an alternative to penicillin for the treatment of infections caused by Gram-positive pathogens such as staphylococci and streptococci.[1] Today macrolides remain valued drugs especially for treatment of respiratory diseases, including community-acquired pneumonia, the leading cause of childhood deaths worldwide due to a Gram-positive pathogen, *Streptococcus pneumonia*,[2−4] as well as pneumonias caused by Gram-negative pathogens such as *Legionella* and *Haemophilus* sp.[5−7]

Macrolides inhibit bacterial protein synthesis by binding at the exit tunnel of the 50S ribosomal subunit and the subsequent abortion of the growth of nascent peptide chains.[8] Four "generations" of macrolides have been introduced into clinical use over the past 50 years, and more are currently in clinical trials, underscoring the importance of this antibiotic class[9,10] (Scheme 1). The later generations are semisynthetic derivatives of progenitor natural products, and their development was a response to a need to improve the pharmacological properties of the natural products and to overcome emerging resistance in pathogens.[11,12]

There are three major mechanisms of macrolide resistance: modification of the 50S target ribosome, active efflux, and enzyme-catalyzed inactivation.[12] The macrolide esterases, EreA[13] and EreB,[14] are members of the last group, and they inactivate drugs through the hydrolysis of the macrolactone ring (Scheme 2). Although less prevalent than modification of the ribosome, resistance via esterase activity has been increasingly reported in clinical isolates across the globe.[15−20]

EreA and EreB are both normally found in integrons and transposons, further raising concern because of the potential ease of gene dissemination.[18,19,21,22] The two enzymes are weakly related with 25% protein sequence identity. EreA is associated with Gram-negative bacteria, while EreB, although originally discovered in *Escherichia coli* on an exogenous plasmid, is thought to originate from Gram-positive organisms on the basis of GC content analysis.[22,23] Preliminary characterization of inactivation products and substrate specificity has been undertaken for both enzymes;[14,24−26] however, no detailed study of the hydrolysis mechanism has been reported.

Here we describe the biochemical characterization of EreB from *E. coli* and EreA from *Pseudomonas stuartii* plasmid DNA utilizing a genomic enzymology strategy.[27,28] This approach suggests that erythromycin esterases comprise a unique family of hydrolases that includes uncharacterized *ere*-homologues from *Bacillus cereus* with known three-dimensional structures, Bcr135 and Bcr136. Through steady-state kinetic analysis,

Received: December 6, 2011
Revised: January 17, 2012
Published: February 3, 2012

   dx.doi.org/10.1021/bi201790u | *Biochemistry* 2012, 51, 1740−1751

Scheme 1

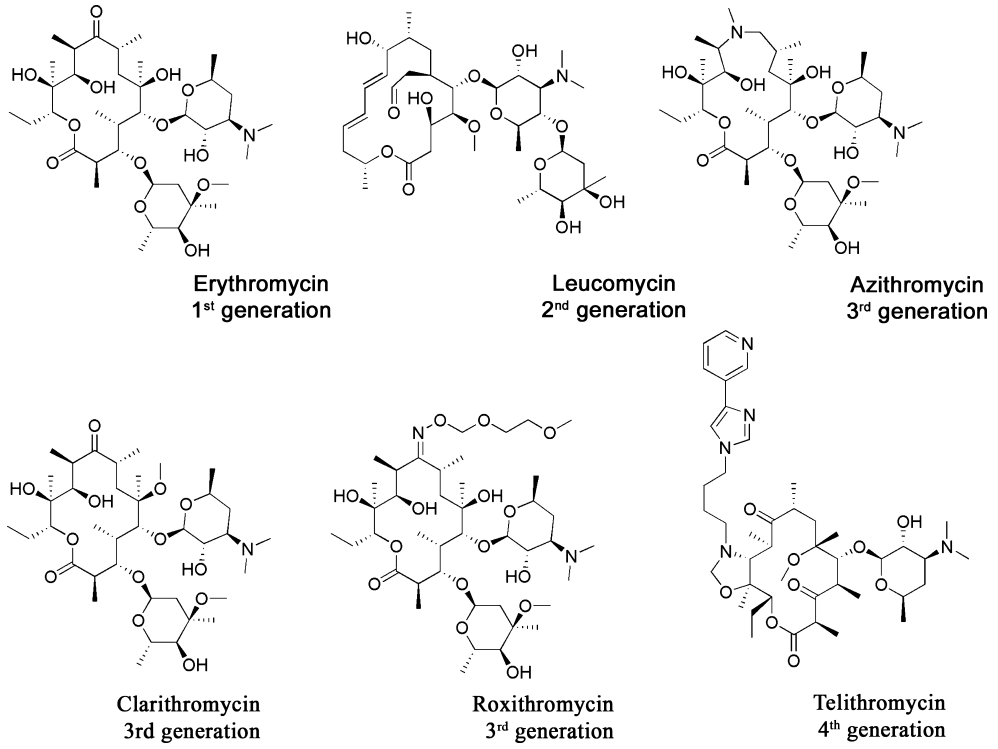

Scheme 2

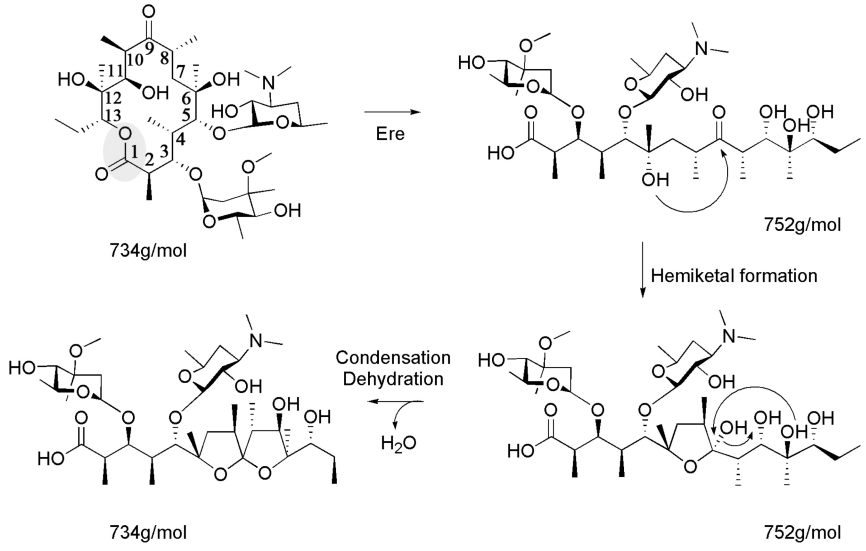

homology-based structure modeling, site-directed mutagenesis, and other studies, we identify the active site region of this enzyme class and compare the biochemical properties of the resistance enzymes with those of Bcr136, allowing commentary on the origins and evolution of macrolide resistance.

EXPERIMENTAL PROCEDURES

Materials. Erythromycin, clarithromycin, azithromycin, and roxithromycin were purchased from Sigma-Aldrich, and working stocks were made in either 100% ethanol (erythromycin and roxithromycin) or DMSO (clarithromycin and azithromycin). Telithromycin was obtained from Aventis Pharmaceuticals Inc. in solid tablet form. Pills containing 5 mg of telithromycin each were crushed using a mortar and pestle and resuspended in 5 mL of 100% ethanol, and insoluble particulates were removed by centrifugation to make a 1 mg/mL stock solution, which was then stored at 4 °C.

Cloning and Mutagenesis of Ere Enzymes. Plasmid DNA containing *ereA* isolated from *P. stuartii* and *ereB* from *E. coli* was generously provided by P. Roy (Université Laval, Sainte-Foy, QC) and P. Courvalin (Institut Pasteur, Paris, France), respectively. Primers for amplification of *ere* genes were designed to include *att* sites to facilitate recombination into Gateway vectors (Invitrogen, Carlsbad, CA) (Table 1 of the Supporting Information). Genes were amplified using polymerase chain reaction, and resulting 1.2 kb fragments were subsequently incorporated into pDONR201 and then pDEST14 Gateway vectors. Plasmids were propagated in *E.*

dx.doi.org/10.1021/bi201790u | *Biochemistry* 2012, 51, 1740−1751

coli Top10 cells. An expression construct for Bcr136 was generously donated by G. Montelione (Rutgers University, Northeast Structural Genomics Consortium).

Site-directed mutations were generated using the QuikChange Mutagenesis Kit (Stratagene). Primers for all genetic manipulations are listed in Table 1 of the Supporting Information. Mutations were verified by DNA sequencing (MOBIX, McMaster University) with the use of plasmid specific primers.

Enzyme Expression. The expression plasmids were transformed into *E. coli* BL21(DE3) cells (Novagen, Darmstadt, Germany) for overexpression under the T7 promoter. Cells were grown in 1 L of Luria-Bertani broth at 37 °C until an optical density of 0.6 at 600 nm was reached. Protein expression was induced overnight at 16 °C by the addition of isopropyl β-D-1-thiogalactopyranoside to a final concentration of 1 mM. Cells were then harvested via centrifugation at 7000*g* using an Avanti J25 centrifuge (Beckman).

Purification of EreA, EreB, and EreB Mutants. Harvested cells were washed in a 0.1% (w/v) NaCl solution and resuspended in 25 mL of buffer A [50 mM HEPES (pH 7.5), 1 M ammonium sulfate, and 2% glycerol (v/v)]. Cells were lysed by sonication with a 20 s pulse followed by a 40 s cooling over 3 min using a $^1/_4$ in. probe (Misonix Ultrasonic liquid processors, XL-2000), and cell debris was removed via centrifugation at 30000*g*. Enzyme purification was a three-part process performed using an AKTA-explorer fast performance liquid chromatography system (GE Healthcare). The course of purification was monitored following absorbance at 280 nm and analyzing peak fractions for the overexpressed protein of the correct size by sodium dodecyl sulfate−polyacrylamide gel electrophoresis.

Cleared lysate was applied to a 30 mL Phenyl Sepharose FastFlow column pre-equilibrated with buffer A. The column was washed with 60 mL of buffer A, and bound proteins were eluted over a 60 mL linear gradient with buffer B [50 mM HEPES (pH 7.5) and 2% (v/v) glycerol], followed by a 30 mL water wash. Ere eluted at 0% ammonium sulfate, and the Ere-containing fractions were pooled and directly applied to a Q-Sepharose HP anion-exchange column equilibrated with buffer B. Bound proteins were eluted with buffer C [50 mM HEPES (pH 7.5), 2% glycerol (v/v), and 1 M NaCl] using a step gradient. Each step consisted of a 10% increase in the level of buffer C with a 15 mL interval between steps. Ere eluted in 30% buffer C. Lastly, Ere-containing fractions from the anion-exchange elution were pooled and applied to a size exclusion HiLoad 26/60 Superdex 200 column equilibrated with buffer D [50 mM HEPES (pH 7.5), 2% (v/v) glycerol, and 150 mM NaCl].

Purification of Bcr136. For Bcr136, expressed as hexahistidine fusion, the cells were lysed at 30K psi using a cell disrupter (Constant Systems) in a lysis buffer consisting of 50 mM HEPES (pH 7.5), 300 mM NaCl, and 1 mM phenylmethanesulfonyl fluoride. The supernatant after cell lysis and centrifugation was applied to a 5 mL Ni-NTA column (QIAGEN). The column was washed with 60 mL of lysis buffer, and protein was eluted with a step gradient using elution buffer [50 mM HEPES (pH 7.5), 250 mM imidazole, and 300 mM NaCl]. Bcr136-containing fractions were pooled and further purified by gel filtration using a HiLoad 26/60 Superdex 200 column equilibrated with buffer D.

All purified proteins were concentrated with an Amicon-Ultra centrifugal device (Millipore) to a range of concentrations between 2 and 20 mg/mL. Protein concentrations were determined using the Bradford assay. The purified proteins were then stored at 4 °C and used within 7 days or frozen with 20% glycerol (v/v) at −20 °C for up to 6 months without loss of activity.

Kirby−Bauer Disk Diffusion Assay. Each purified esterase was tested for its ability to inactivate the following panel of macrolides: erythromycin, azithromycin, clarithromycin, telithromycin, and roxithromycin. The enzyme (2 nmol) was incubated with the macrolide (30 μM) for 1 h at 24 °C; the reaction was stopped via addition of methanol to a final concentration of 50% (v/v), and samples were clarified by centrifugation. A Kirby−Bauer biological disk assay was used to assess inactivation.[29] Macrolide susceptible *Micrococcus luteus* was used as the indicator organism, and antibiotic alone and a buffer/methanol mixture were used as controls. A volume of 10 μL of reaction mixture or control was spotted onto sterile paper disks placed on an LB plate spread with *M. luteus*. Zones of inhibition were scored after samples had grown for 2 days.

Enzyme Product Characterization by Liquid Chromatography and Mass Spectrometry (LC−MS). LC−MS was used to detect the inactivation products of macrolides by EreA and EreB, using an Agilent 1100 Series LC system (Agilent Technologies Canada, Inc.) and an Applied Biosystems (Boston, MA) QTRAP LC/MS/MS instrument. Reaction mixtures (50 μL) consisting of 2 nmol of Ere with 30 μM macrolide were incubated at room temperature for up to 24 h. Reactions were stopped via the addition of 3 volumes of cold acetonitrile and mixtures placed on ice for 5 min and then clarified by centrifugation. Analysis of the erythromycin inactivation products was achieved via reverse phase LC using a C18 column (Dionex, Acclaim120, 3 μm, 120 Å, 4.6 mm × 150 mm), a Dionex GP40 gradient pump system, and the following method: 5% solvent B from 0 to 5 min, a 5 to 25 min linear gradient up to 97% solvent B, 5% solvent B from 25 to 28 min, 0.05% formic acid (v/v) (solvent A), acetonitrile with 0.05% (v/v) formic acid (solvent B), and a flow rate of 1 mL/min. For clarithromycin and roxithromycin, the method used was essentially the same, the only difference being that the linear gradient to 97% solvent B occurred over 20 min.

Ere Modeling. *E. coli* EreB and *P. stuartii* EreA sequences were input into the PSIPRED Protein Structure Prediction Server,[30] and the profile−profile prediction method with secondary structure, pGENthreader, was used to search for Ere structural homologues. The predicted top three structural homologues for both proteins are listed in Table 2 of the Supporting Information. The sequence alignments generated by pGENthreader predicted the highest level of fold similarity for both EreA and EreB with two structures: Protein Data Bank (PDB) entries 3b55 and 2qgm. The alignments with these two structures and their atom coordinates were used to make the Ere structural homology models. Modeler 9v7, a program for comparative protein structure modeling by satisfaction of spatial restraints, was used for this purpose.[31] The script file was generated by using a model-default.py input file as a template with the default settings.

[^{14}C]Erythromycin Inactivation Assay. Radiolabeled erythromycin was used in combination with thin-layer chromatography (TLC) to detect products and reactants of the reaction catalyzed by erythromycin esterases. In each 50 μL reaction mixture, erythromycin (21−4320 μM) containing 4.0 × 10^{-3} μCi of [^{14}C]erythromycin was incubated with 0.025−10.3 nmol of enzyme for 4−30 min. The wide range of the

Table 1. Activity of Erythromycin Esterase Superfamily Enzymes against a Panel of Macrolides[a]

Ere	erythromycin	clarithromycin	roxithromycin	azithromycin	telithromycin
EreA	+	+	+	−	−
EreB	+	+	+	+	−
Bcr136	−	−	−	−	−

[a]A plus indicates the ability to completely inactivate a 50 μL reaction mixture of 100 μM drug after incubation for 1 h with 0.08 mg of purified protein, as determined by the Kirby−Bauer disk diffusion assay.

amount of enzyme added to the reaction mixture and times of incubation was due to various activity levels of wild-type and mutant enzymes. The reaction was stopped via the addition of 50% methanol; 4.5 μL of each reaction mixture was applied to a silica gel plate (Alugram SILG, UV254, Mackerey-Nagel). The plate was then developed for 20 min in a pre-equilibrated TLC chamber using a 50:50 methanol/chloroform mixture as the solvent system and analyzed with a Typhoon variable mode imager. ImageQuant version 5.2 was used to quantify the relative radioactive intensity. Grafit version 4.0.21 was used to determine kinetic parameters, with initial rates determined using eq 1 and the nonlinear least-squares method (Erithacus Software, Staines, U.K.).

$$v = (k_{cat}/E_t)[S]/(K_M + [S]) \quad (1)$$

***p*-Nitrophenyl Butyrate Enzyme Assay.** Esterase activity was measured using a spectrophotometric assay with *p*-nitrophenyl butyrate (*p*-NPB) as the substrate. A 96-well plate format assay was adapted from previously described conditions.[32] Each 250 μL reaction mixture contained 50 mM HEPES (pH 7.5), 0.2% Triton X-100 (Sigma), and 3−5 nmol of purified esterase protein. Reactions were initiated via addition of 15.6−2000 μM *p*-NPB and monitored at 405 nm for 45 min. The amount of reaction product released (*p*-nitrophenol) was calculated on the basis of a prepared standard curve of *p*-nitrophenol under assay conditions.

pH Profile. The dependence of kinetic parameters on pH was determined for EreA and EreB with the use of the continuous spectrophotometric assay and *p*-NPB as the substrate. The following buffer systems were used, each at 50 mM: MES for pH 6.0−6.5, MOPS for pH 6.5−7.5, HEPES for pH 7.0−8.0, and TAPS for pH 8.0−9.0. Standard curves were prepared for the absorbance of known concentrations of the colored product *p*-nitrophenol at 405 nm under each buffer condition, to allow for conversion of absorbance to product concentration. Data were analyzed by the nonlinear least-squares method, and fit to eq 1 (above) with Grafit. Kinetic parameters were then fit to eq 2 or 3 using Gnuplot (version 4.2.5), where Y is the varied parameter (V_{max} in eq 2 and V_{max}/K_M in eq 3), C is the limiting value of this parameter, $[H^+]$ is the concentration of hydrogen ions, and K_1 and K_2 are the ionization constants.

$$Y = C/(1 + [H^+]/K_1) \quad (2)$$

$$Y = C/(1 + [H^+]/K_1 + K_2/[H^+]) \quad (3)$$

Solvent Isotope Effect. The solvent isotope effect on the hydrolysis reactions conducted by the erythromycin esterases was examined using both the [^{14}C]erythromycin end point assay and the *p*-NPB continuous assay in the presence of either water or D_2O. The [^{14}C]erythromycin assay was performed as described above with the following difference: a 20× buffer [3 M NaCl, 1 M HEPES (pH 7.5), and 20 mM EDTA] was prepared and diluted accordingly in either H_2O or D_2O. The pH stability of the diluted buffer was verified using pH paper, and in these reactions, D_2O comprised 85% of the solvent. The *p*-NPB experiments were set up as described, and in these reactions, D_2O accounted for 84% of the solvent present. Standard curves with the reaction product *p*-nitrophenol were prepared fresh in reaction buffer containing D_2O to correct for any change in absorbance at 405 nm that may occur because of the change in solvent. Data were analyzed as before, and kinetic parameters for D_2O-containing reaction mixtures were compared with those obtained for each enzyme in H_2O.

Inhibition of EreA, EreB, and Bcr136. The effects of known hydrolase inhibitors on EreA, EreB, and Bcr136 were examined. The spectrophotometric assay with *p*-NPB was used to quantify the extent of inhibition by comparing the enzyme activity in the presence and absence of the inhibitor. All reactions were initiated with 2 mM *p*-NPB; enzyme concentrations were 0.2 mg/mL for EreA and 0.5 mg/mL for EreB and Bcr136. Ser/Cys/Thr hydrolase inhibitors 4-(2-aminoethyl)benzenesulfonyl fluoride (AEBSF, 1 mM), chymostatin (100 μM), and leupeptin (10 μM) were used, with the final concentration of the inhibitor indicated in parentheses. Metallohydrolase inhibitors ethylene glycol tetraacetic acid (EGTA) and phenanthroline were used at a final concentration of 5 mM.

Chelex 100 resin (Bio-Rad) was used to examine the effects of this resin on enzyme activity. The resin (∼20 mg) was washed with water and added to 200 μL of enzyme solution, and this slurry was incubated for 2 h at 4 °C. The slurry was then packed in a column with the retention of the liquid fraction. Additionally, the liquid fraction was passed through fresh resin four times, and then the enzyme activity was quantified using the *p*-NPB continuous assay.

In Vivo Macrolide Inactivation. Minimal inhibitory concentrations for *E. coli* BL21(DE3) cells harboring the various erythromycin esterase enzymes were determined by the broth dilution method in LB broth. Colonies of *E. coli* cells harboring expression plasmids for each protein were resuspended in a 0.85% sterile saline solution to an OD_{600} of 0.08. This solution was diluted 1/:10 in sterile LB broth twice, to a final dilution of 1:100; 50 μL of this cell suspension was added to sterile 96-well plates containing 50 μL dilutions of erythromycin in LB broth ranging from 8 to 2048 μg/mL. Plates were incubated at 37 °C overnight, and the MIC was defined as the lowest concentration of drug having no growth present after 16 h.

RESULTS

Substrate Specificity of the Purified Esterase Proteins. Both EreA and EreB inactivated the natural product erythromycin as determined by a bioassay measuring residual antibiotic activity. Furthermore, EreB was able to inactivate all macrolides in our panel with the exception of the ketolide telithromycin (Table 1). EreA was also unable to inactivate telithromycin; additionally, EreA did not recognize the

dx.doi.org/10.1021/bi201790u | *Biochemistry* 2012, 51, 1740−1751

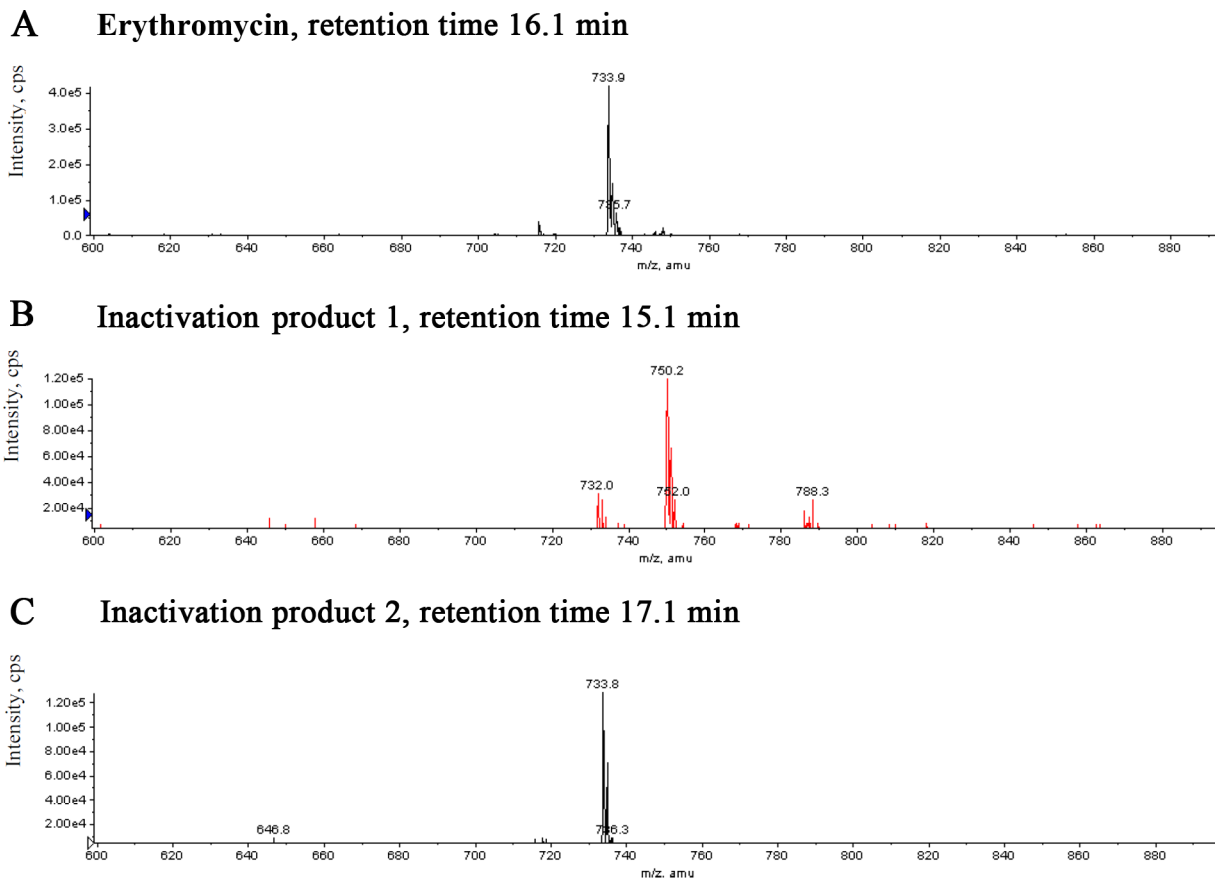

Figure 1. LC−MS profiles for intact and EreB-inactivated erythromycin. (A) MS trace in positive ion mode for erythromycin, with a retention time of 16.1 min. (B) MS trace in negative ion mode for hydrated inactivation product **1**, with a retention time of 15.1 min. (C) MS trace in positive ion mode for dehydrated inactivation product **2**, with a retention time of 17.1 min.

semisynthetic drug azithromycin. This broader substrate specificity observed for EreB is consistent with previous reports.[16,22,26] Bcr136 was unable to inactivate any of the macrolides.

Characterization of Enzymatic Inactivation Products. The products of macrolide inactivation by EreA and EreB were analyzed by LC−MS, confirming that the loss of antimicrobial activity seen in the bioassay was the result of inactivation through hydrolysis. Previous work has shown that after enzyme-catalyzed lactone ring opening of erythromycin, a nonenzymatic intracellular hemiketal is formed between the hydroxyl at C6 and the ketone at C9, which is followed by condensation and dehydration of the macrolide backbone. In our analysis, masses corresponding to all expected products of the erythromycin inactivation were detected (Table 3 of the Supporting Information).[14] With reactions catalyzed by Ere enzymes, there was a clear difference between a retention time of 16.1 min and a mass-to-charge ratio (m/z) of 734 for erythromycin in the absence of enzyme, the unhydrolyzed substrate, and a retention time of 17.1 min and an m/z of 734 for erythromycin in the presence of enzyme, assumed to correspond to the previously described nonenzymatic dehydration product of erythromycin hydrolysis. It was also seen that these two compounds having the same mass but eluting at different times appear to ionize differently, with negative ions having an m/z of 734 being detected only in the sample incubated with enzyme (Figure 1).

EreA and EreB yielded indistinguishable products as per our LC−MS analysis. The inactivation product of the EreB reaction with clarithromycin, which has a hydroxymethyl group at position C6 and thus is unable to undergo subsequent nonenzymatic transformations, as well as the inactivation product of roxithromycin due to ring hydrolysis, rather than the formal possibility of initial hydrolysis of the imine at position C9 generating erythromycin, and subsequent inactivation, was also verified by LC−MS (Table 3 of the Supporting Information). To the best of our knowledge, this is the first report of the inactivation product characterization for EreB-mediated clarithromycin and roxithromycin hydrolysis. LC−MS was additionally used to detect possible hydrolysis of erythromycin in reactions with purified Bcr136; however, no activity was observed, confirming our bioassay studies that show that this enzyme is not a macrolide esterase.

Structural Characteristics of the Erythromycin Esterase Protein Superfamily. Protein BLAST analysis shows that neither EreA (44.7 kDa) nor EreB (48.2 kDa) shares sequence homology with any of the biochemically characterized hydrolases. Instead, they form a unique superfamily designated as the "erythromycin esterase superfamily" by the National Center for Biotechnology Information.[33] This superfamily includes proteins annotated as succinoglycan biosynthetic proteins; this annotation, however, has not been experimentally verified, and their exact function remains unknown. Nevertheless, two such homologues, Bcr135 (51.1 kDa) and Bcr136 (50.5 kDa), from *B. cereus*, have been structurally characterized, and the structures have been deposited in the PDB. The structures of these proteins, homologous to each other in primary (37% identical and 56% similar) and tertiary structure, are the result

dx.doi.org/10.1021/bi201790u | *Biochemistry* 2012, 51, 1740−1751

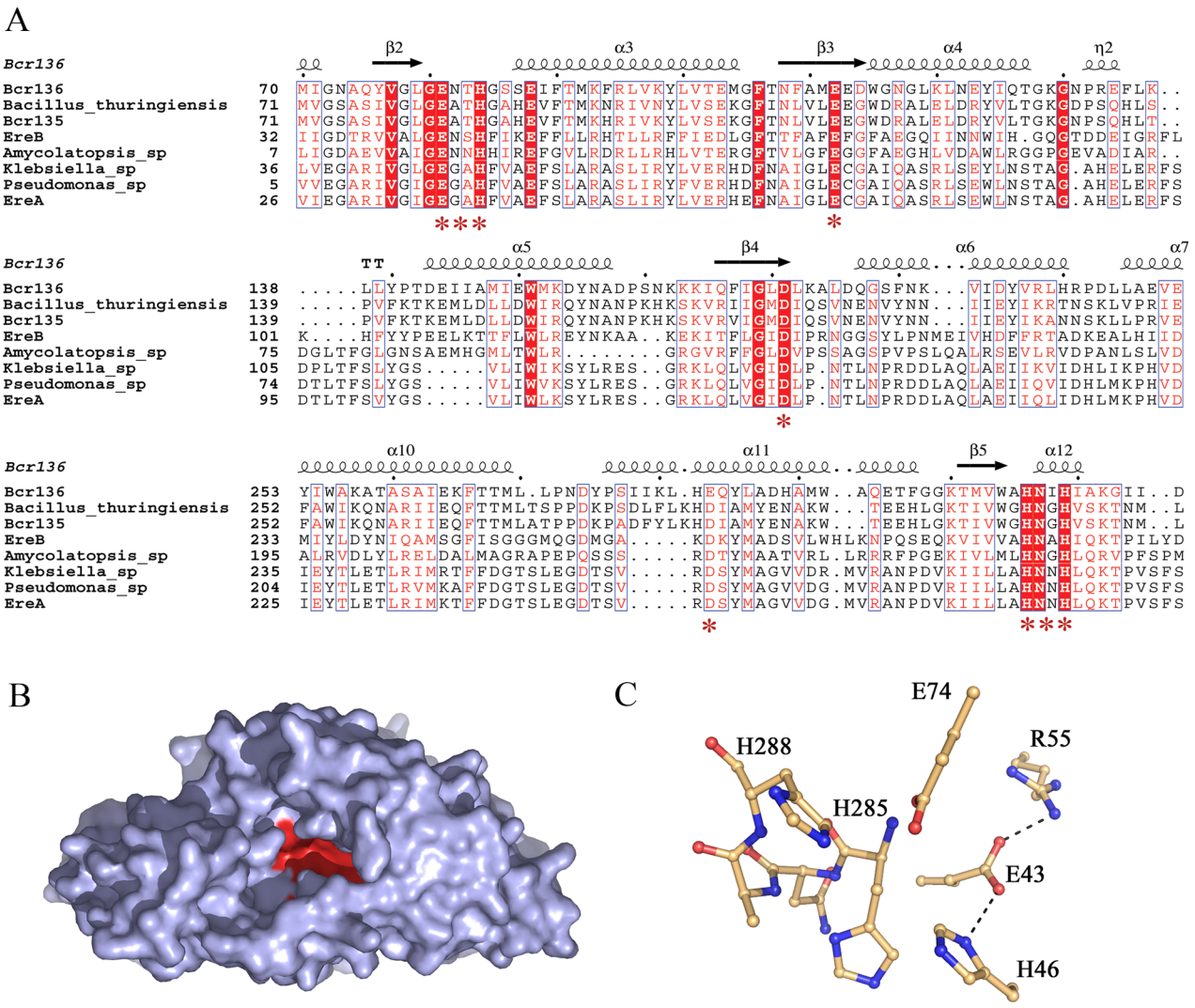

Figure 2. Analysis of the primary and tertiary structure of the erythromycin esterase enzyme superfamily. (A) Partial sequence alignment for the erythromycin esterase enzymes. The full alignment was generated by MUSCLE and EspRIPT and truncated in the figure only for the sake of conciseness. Residues highlighted in red are strictly conserved, and those colored red are functionally conserved. Secondary structural elements of Bcr136 are superposed on top of the alignment, and asterisks mark residues in the active site pocket. (B) Surface representation of the Bcr136 structure (gray) highlighting the strictly conserved residues in the active site cleft in red. (C) Close-up of the active site of the erythromycin esterase enzymes represented by the EreB model.

Table 2. Quantification of Esterase Activity As Shown by Steady-State Kinetic Parameters As Determined with [^{14}C]Erythromycin and *p*-NPB Assays

	erythromycin hydrolysis			*p*-NPB hydrolysis		
enzyme	k_{cat} (s^{-1})	K_M (μM)	k_{cat}/K_M (s^{-1} M^{-1})	k_{cat} (s^{-1})	K_M (μM)	k_{cat}/K_M (s^{-1} M^{-1})
EreB						
WT	3.8 ± 0.2	210 ± 46	2×10^4	17.1 ± 0.2	280 ± 12	6×10^4
E43A	0.7 ± 0.03	124 ± 16	6×10^3	2.8 ± 0.2	1700 ± 220	2×10^3
H46A	0.0071 ± 0.0004	210 ± 44	30	0.55 ± 0.03	1100 ± 250	5×10^2
E74A		no activity		5.1 ± 0.2	480 ± 53	1×10^4
H285A	17.3 ± 0.5	980 ± 64	2×10^4	8.8 ± 0.3	650 ± 47	1×10^4
H288A	0.0032 ± 0.0003	180 ± 55	20	14.2 ± 1.3	1080 ± 21	1×10^4
EreA	1.6 ± 0.1	280 ± 38	6×10^3	140 ± 8	150 ± 15	9×10^4
Bcr136		no activity		34.1 ± 1.9	900 ± 110	4×10^4

of unpublished work by the Northeast Structural Genomics Consortium.

EreA is 16 and 25% identical in sequence (36 and 39% similar) and EreB is 21 and 24% identical in sequence (40 and 43% similar) with Bcr135 and Bcr136, respectively. Sequence alignment generated by MUSCLE[34] reveals conserved regions spanning both Ere and Bcr family members (Figure 2A). Interestingly, 53% of the strictly conserved residues cluster

dx.doi.org/10.1021/bi201790u | *Biochemistry* 2012, 51, 1740−1751

within a cleft formed by two domains of the Bcr135 and Bcr136 structures, pointing to the potential active site location (Figure 2B). Furthermore, the ability of Bcr136 to act as an esterase (described below) ascertains that the relationship between Ere and Bcr enzymes extends beyond structural homology and encompasses function, as well.

These observations allowed us to use the Bcr structures for Ere homology modeling. The models produced by Modeler were in good agreement with the primary structure alignments. The insertions found in both EreA and EreB sequences were located in loop regions and did not appear to disrupt the secondary structural elements or the conservation of the overall fold. The differences between EreA and EreB models were minimal and also restricted to short insertions in the loop regions. Strictly conserved residues E43, H46, E74, H285, and H288 (*E. coli* EreB numbering) in the active site cleft, with the latter two being part of a conserved HNXH motif, were hypothesized to be catalytically significant (Figure 2). To further validate the active site location and to probe the catalytic mechanism, site-directed mutagenesis of these five residues in EreB was performed.

Enzyme Kinetics Determined via the [^{14}C]-Erythromycin Assay. The results for the enzymatic hydrolysis of radioactive erythromycin are summarized in Table 2. As expected, EreA and EreB are both capable of erythromycin hydrolysis, with similar catalytic efficiencies of $\sim 10^4$ s^{-1} M^{-1}. The Michaelis constant (K_M) in the midmicromolar range and turnover number values (k_{cat}) of 2−4 s^{-1} are comparable for the two enzymes but much lower than those for EreA purified from *Pseudomonas* sp. reported by Kim et al.[26] While the reason for this is not clear, several major contributing factors include organism specific variability, effects of recombinant expression, and possible metal dependence (see below). Despite the homology to erythromycin esterases, Bcr136 was unable to inactivate the antibiotic.

Site-directed mutagenesis was performed on the conserved residues of the EreB active site. Only the E74A mutation completely abolished activity under our assay conditions, while the H46A and H288A mutations reduced the k_{cat} ~1000-fold. The substantial differences between the wild-type and mutant enzyme activities serve to confirm our structural predictions and active site identification. The H285A mutation led to a 5-fold increase in the K_M for erythromycin, while the k_{cat} was virtually unaffected.

Enzyme Kinetics Determined via the *p*-NPB Assay. The model ester *p*-NPB was found to be an effective substrate for both EreA and EreB. The catalytic efficiency (k_{cat}/K_M) of the two enzymes is very similar, at $\sim 10^5$ s^{-1} M^{-1}, although the turnover number (k_{cat}) for EreA is 10-fold higher than that of EreB. The lower catalytic activity of EreB could potentially be correlated with the broader substrate specificity observed for this enzyme. Structural characterization of the Ere enzymes complexed with substrates will clarify if this is the case.

Of the predicted active site residues from Ere modeling, all EreB mutants showed a decrease in the substrate affinity, with K_M values increasing 2−4-fold. The H46A mutant showed a marked decrease (100-fold) in catalytic efficiency, while mutation of E43, which forms a hydrogen bond with H46, to an alanine resulted in a 10-fold reduction. Mutations of H288 and E74 to alanine had little effect on the catalytic efficiency of EreB with respect to *p*-NPB hydrolysis. These observations contrast the results of the erythromycin assay, where the hydrolase activity was drastically reduced for both H288A and E74A mutants, and thus point to an important role for these residues in macrolide specificity rather than direct ester hydrolysis. The difference may also reflect the reactivity of the two substrates with *p*-NPB being highly activated and readily hydrolyzed in comparison to erythromycin. Bcr136 was also able to use *p*-NPB as a substrate, even though it is unable to hydrolyze any of the macrolide antibiotics tested (Table 2). This confirmed our hypothesis based on sequence and structural similarity that Bcr136 is an esterase.

In Vivo Inactivation of Macrolides. *E. coli* cells expressing each of the different expression constructs for the erythromycin esterases were tested for their ability to grow in the presence of erythromycin. Cells expressing EreA and EreB showed increased MIC values when compared to the empty vector control (Table 3). It was found that these increased MIC's were consistent with the ability of these proteins, when purified, to inactivate erythromycin and other macrolides. Mutations

Table 3. MIC Values of Erythromycin against *E. coli* BL21(DE3) Cells Containing Expression Plasmids for EreB and Its Mutants, EreA, and Bcr136

enzyme	MIC (μg/mL)
empty vector	63
EreB	
WT	1000
E43A	125
H46A	63
E74A	63
H285A	1000
H288A	63
EreA	1000
Bcr136	63

H288A, H46A, and E74A, which showed a marked decrease in erythromycin esterase function for the EreB enzyme, displayed MIC values comparable with the empty vector negative control, while the active H285A mutant exhibited that of the wild-type enzyme. The E43A mutation showed an intermediate resistance phenotype fully consistent with the in vitro observations.

pH Dependence of Steady-State Rates. Examination of the pH dependence of the kinetic parameters can infer the participation of particular residues important for catalysis, based on their ionization constants.[35] The pH dependence of k_{cat} for EreA indicated a single pK_a value of ~6.2, suggesting that the enzyme may employ a catalytic histidine residue (Figure 1 of the Supporting Information).[36] Plotting the dependence of k_{cat}/K_M on pH generated a bell-shaped curve with two ionization constants, a pK_a of 5.6 and a pK_b of 9.1. The pK_a of 5.6 is consistent with the importance of a deprotonated histidine residue. The additional role of a residue with a pK_a of 9.1 requires further investigation. No significant pH dependence of rate constants was measured with EreB. This may be the result of practical constraints of the assay; *p*-NPB undergoes substantial nonenzymatic hydrolysis below pH 6.0, which may mask the effects of pH on EreB hydrolysis rates, as this enzyme is not as efficient as EreA. Alternatively, this observation may reflect some differences between the residues used for catalysis in EreA and EreB.

Solvent Isotope Effects (SIE). Using the [^{14}C]-erythromycin assay, turnover values for the reactions conducted in D_2O and H_2O were identical for both EreA and EreB. SIE

dx.doi.org/10.1021/bi201790u | *Biochemistry* 2012, 51, 1740−1751

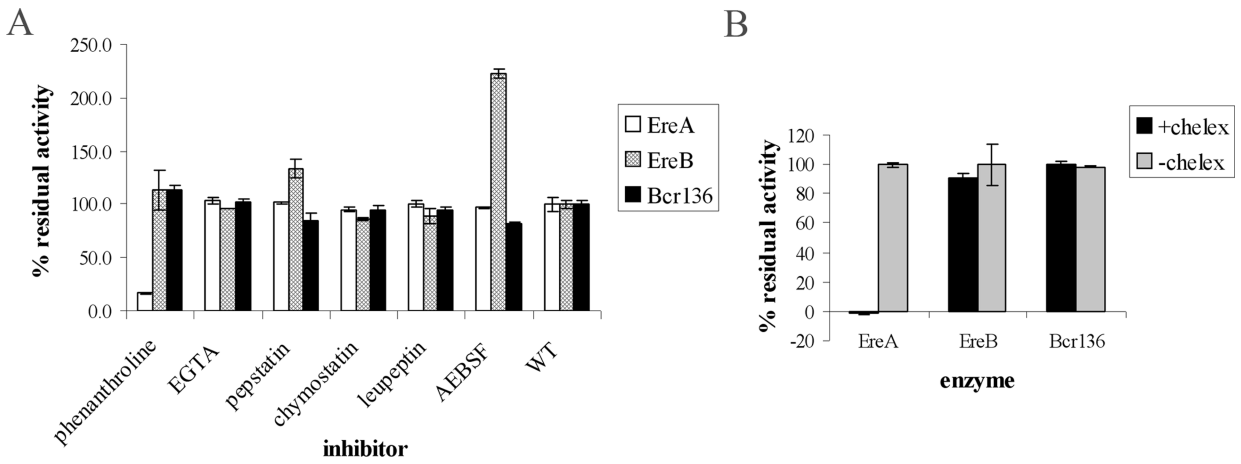

Figure 3. Biochemical profiles for EreA, EreB, and Bcr136. Graphs are used to show the residual activity of the enzymes assayed against (A) hydrolase inhibitors and (B) Chelex 100.

analysis using the *p*-NPB assay and EreA as the catalyst showed that the k_{cat} value was only 1.43 times larger in the H_2O solvent than the value when the reaction was conducted in D_2O. For EreB, a slightly larger SIE of 2.15 was measured.

Hydrolase Inhibitor Profiles. Because none of the three enzymes characterized in this work (EreA, EreB, or Bcr136) shares sequence homology with any known family of hydrolases, a panel of well-characterized Ser/Thr, Cys, and metallohydrolase inhibitors was used to explore potential mechanisms (Figure 3A). EreA was inhibited by a chelating agent, phenanthroline, indicating a metal requirement for EreA activity, while neither EreB nor Bcr136 showed any significant inhibition. The metal requirement was validated through Chelex 100 experiments, showing again that EreA was inhibited while EreB and Bcr136 were unaffected (Figure 3B). Interestingly, EreB is activated by AEBSF; however, the reason for this phenomenon remains unclear.

DISCUSSION

Erythromycin Esterases Form a Unique Superfamily of Hydrolases. Erythromycin esterase genes are widespread in microorganisms;[15−20] however, little is known about their enzymatic function.[26] Primary and tertiary structural analysis shows that erythromycin esterases are not related to known hydrolases; they form a unique superfamily, and the catalytic mechanism for these enzymes remains uncharacterized. This is the first report to focus on the catalytic features and potential origins for the erythromycin esterase superfamily by means of biochemical analysis for three of its members: two bona fide drug resistance enzymes, EreA and EreB, and a homologue of unknown function encoded in the genome of *B. cereus*, Bcr136.

Ere Mechanism. There is a tremendous body of literature about enzyme-catalyzed hydrolytic reactions. As EreA and EreB specialize in hydrolysis of lactones, their connection with the lactonase subgroup of hydrolases was examined. This group appears to have been formed by convergent evolution. Mammalian paraoxonases are β-propellers;[37] bacterial phosphotriesterase-like lactonases are $(\alpha\beta)_8$ barrels,[38,39] and quorum-quenching lactonase is an $\alpha\beta/\beta\alpha$ sandwich.[40] Therefore, the new fold represented by erythromycin esterases adds additional diversity to the enzyme class.

Despite great structural diversity, the general agreement is that four major components are required for enzyme-catalyzed ester hydrolysis: (1) a nucleophile attacking the carbonyl, (2) a general base to activate the nucleophile, (3) an electrophile for carbonyl polarization, and (4) a proton donor for protonation of the leaving group.[41,42] The nucleophile for the erythromycin esterases is unlikely to be of the Ser/Thr/Cys hydrolase class as there are no suitable conserved residues in the active site; common Ser/Cys/Thr hydrolase inhibitors are ineffective against these enzymes, and no covalent enzyme intermediates or burst kinetics were detected (data not shown).

The alternative nucleophile is a water molecule, activated by a general base. This scenario is consistent with the data generated for both EreA and EreB enzymes. H46 of EreB is the most fitting candidate for the general base role, as it is strictly conserved, forms a hydrogen bonding pair with a conserved acidic residue (E43 in EreB), and is the only residue whose mutation affects both erythromycin and *p*-NPB hydrolysis in our analysis with a 1000-fold reduction in erythromycin hydrolysis activity and a 100-fold reduction for that of *p*-NPB (Table 2). The observation of residual *p*-NPB hydrolysis is potentially due to the fact that it is a highly activated substrate. The E43A mutation also affected both activities, further underscoring the importance of this residue pair in catalysis. Consistent with this hypothesis is the EreA pH profile, with a pK_a of 5.6 indicative of a general histidine base. A negligible SIE effect was observed for both Ere enzymes, indicating that nucleophilic attack by water is not rate-limiting. Further investigation of the mechanisms for both EreA and EreB is needed to gain more insight into the mechanistic details of this hydrolysis reaction. Especially useful would be structural characterization of the active sites in the presence of a substrate.

Comparison of Erythromycin Esterase Biochemical Profiles. EreA and EreB are clearly distinct from each other. While antibiotic inactivation products are the same for both enzymes, the EreB substrate profile is substantially broader than that for EreA, and this enzyme is able to metabolize not only the natural product erythromycin but also semisynthetic derivatives, including the widely used azalide azithromycin (Zithromax). Neither Ere enzyme though can hydrolyze the ketolide telithromycin. Besides substrate specificity, the two enzymes also have different esterase inhibitor susceptibilities, with EreA showing sensitivity to metal chelators, whereas EreB and the structural analogue Bcr136 appear to be resistant. The latter two in fact were not inhibited by any of the tested hydrolase inhibitors.

dx.doi.org/10.1021/bi201790u | *Biochemistry* 2012, 51, 1740−1751

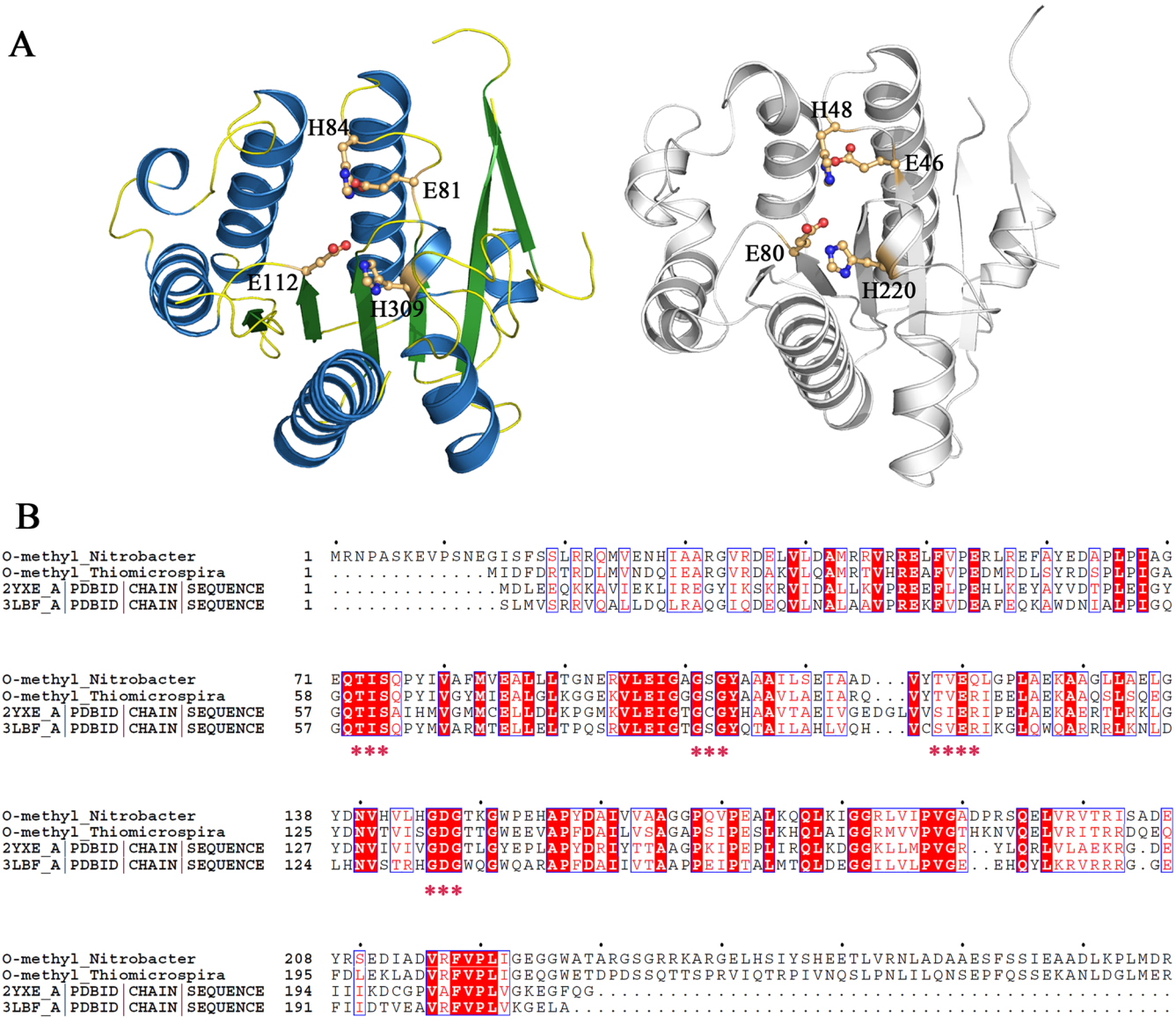

Figure 4. Physiological function of Bcr136. (A) Comparison of the structural core of Bcr136 (colored by secondary structure) and that of the heme-binding protein (PDB entry 2G5G, colored gray). The conserved active site residues are shown in ball-and-stick representation (colored wheat). (B) Sequence alignment of the N-terminal domain of bifunctional Ere PIMTs with PIMTs of known structure. The color coding is the same as in Figure 2B.

Nevertheless, our kinetic, mutagenesis, and modeling studies show that the three enzymes are united by a common hydrolase function and a conservation in the fold and active site architecture despite the relatively weak homology at the primary sequence level. This confirmation of structure–function homology argues against the possibility of a different catalytic mechanism for the three enzymes, as a proposition of structurally related enzymes catalyzing the same reaction via a different mechanism would be highly unusual. It is formally possible that EreB and Bcr136, like EreA, are metalloenzymes, because examples of metal-dependent hydrolases resistant to chelating agents exist.[49] The metal would then function as the electrophile, still consistent with our data pointing to a nucleophilic water and a histidine general base. We attempted to characterize any highly tightly bound metals by inductively coupled plasma mass spectrometry and X-ray absorption spectroscopy for both EreA and EreB with nonconclusive results. Altogether, the lack of evidence of the presence of a metal in EreB and Bcr136 enzymes leads to our parsimonious prediction that Ere enzymes do not require a metal ion for catalysis. Therefore, the metal dependence of EreA is likely the result of a unique structural requirement rather than a general mechanistic one. Only small insertions in the loop regions differentiated the structural model of EreA from that of EreB, providing little information regarding the possible location of this metal binding site; its full characterization awaits structure determination.

Origins of Erythromycin Esterases. Bcr136 possesses no erythromycin esterase activity but shows clear structural homology with Ere proteins and is capable of ester hydrolysis. In an effort to elucidate the cellular function of Bcr136, a search for structural homologues using DALI[43] was performed and yielded only one structure (PDB entry 2G5G) with a similar core fold and a root-mean-square deviation of 3.2 Å^2 (Figure 4A). This structural homologue has been reported to be involved in heme transport and offers no obvious connection

dx.doi.org/10.1021/bi201790u | *Biochemistry* 2012, 51, 1740–1751

with esterases.[44] It is interesting to note that all of the EreB conserved residues, except the dispensable His285, are present in this structure. Whether nature uses this structural motif for a wide range of functions, like the $(\beta\alpha)_8$ barrels, for example,[45] leading to a high degree of divergence, will become clear as more structures of the same fold become available.

Comparative analysis of the primary sequences of the members of the erythromycin esterase superfamily using the NCBI-BLAST server yielded another interesting observation: homology with a bifunctional enzyme found in a number of organisms. Here the esterase domain is in the C-terminal region of the protein and fused to an N-terminal protein isoaspartyl *O*-methyltransferase (PIMT) gene. In PIMT−Ere bifunctional proteins, the sequence identity for the PIMT domain is ∼42% (Figure 4B), and that for Ere is ∼23% when it is compared to characterized proteins. The sequence identity of the two domains with characterized enzymes leaves no doubt that the homology is real and provides yet another clue about the physiological function of Bcr136.

PIMT is a ubiquitous enzyme whose physiological function is not fully understood. It utilizes *S*-adenosylmethionine in repair of deamidated asparagine sites (Scheme 3) and is also implicated in cell signaling.[46−48] The product of the PIMT reaction, the succinamidyl moiety, is thought to convert

Scheme 3[a]

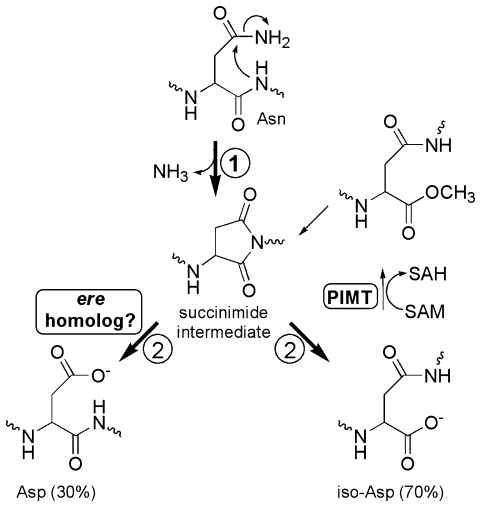

[a]Adapted from ref 46.

nonenzymatically to an aspartate or to revert back to the isoaspartate.[49] We hypothesized that an Ere-like esterase could potentially drive the succinamide intermediate hydrolysis to the wanted aspartate product.

N-Methylsuccinamide (NMS), used as an analogue for this intermediate, was incubated with Bcr136, and potential products of this enzyme reaction were compared with those from chemical hydrolysis of NMS using LC−MS analysis (data not shown). We determined that NMS is not a substrate for Bcr136: this could mean either that Bcr136 is not involved in PIMT intermediate hydrolysis or that the full protein substrate is required for recognition and the truncated NMS analogue is not accepted.

Conclusion. The course that pathogenic organisms will take in developing antibiotic resistance is unpredictable. It is certain, however, that novel as well as currently rare resistance mechanisms will continue to surface. To preempt resistance in the clinics, understanding of current mechanisms as well as continuous exploration of the depths of the antibiotic resistome is needed. In this report, we describe the characterization of macrolide antibiotic esterases, EreA and EreB, and that of a homologous esterase, Bcr136. These enzymes are shown to comprise a novel "erythromycin esterase" superfamily of hydrolases. Collectively, structural information, kinetic analysis, mutagenesis, inhibitor profiling, and pH and SIE studies provide the following insights into catalytic features for the superfamily members. The active site was identified, and a Ser/Cys/Thr-mediated hydrolysis was ruled out (Figure 2). Instead, EreA and EreB are proposed to utilize a His-Glu pair for the nucleophilic activation of water. The physiological role of Bcr136, identified as an esterase in this study, remains unclear; however, the genomic enzymology approach provides clues for potential connections (Figure 4 and Scheme 3) and paves the way for further experiments.

Significance. This is the first study to examine the mechanistic details of enzymatic hydrolysis of the clinically important macrolide antibiotics. The biochemical analysis led to expansion of the hydrolase enzyme superfamily as the erythromycin esterase class was found to be unique. Therefore, this work contributes not only to the efforts toward antibiotic resistance reversal in the clinic, where knowledge of resistance enzyme mechanisms is essential for drug design, but also to our fundamental understanding of enzyme function in a genomic context.

■ ASSOCIATED CONTENT

Supporting Information

Primers used for *ere* gene amplification and mutagenesis (Table 1), fold predictions for EreA and EreB modeling (Table 2), LC−MS analyses of Ere-generated macrolide inactivation products (Table 3), profiles for the dependence of EreA catalytic rates on pH (Figure 1). This material is available free of charge via the Internet at http://pubs.acs.org.

■ AUTHOR INFORMATION

Corresponding Author

*Phone: (905) 525-9140, ext. 20230. E-mail: wrightge@mcmaster.ca.

Author Contributions

M.M. and K.P. contributed equally to this work.

Funding

This research was supported by the Canadian Institutes of Health Research (MT-13536) and the Canada Research Chairs program (G.D.W.).

Notes

The authors declare no competing financial interest.

■ ACKNOWLEDGMENTS

We thank Dr. Paul Roy for his generous gift of *ereA*, Dr. Patrice Courvalin for *ereB*, and Dr. Gaetno Montelione for *Bcr136* plasmid DNA. Dr. Pawel Grochulski is gratefully acknowledged for performing EreA and EreB X-ray absorption scans.

■ ABBREVIATIONS

NMS, *N*-methylsuccinamide; LC−MS, liquid chromatography and mass spectrometry; *p*-NPB, *p*-nitrophenyl butyrate; AEBSF, 4-(2-aminoethyl)benzenesulfonyl fluoride; EGTA, ethylene glycol tetraacetic acid.

REFERENCES

(1) Blondeau, J. M. (2002) The evolution and role of macrolides in infectious diseases. *Expert Opin. Pharmacother. 3*, 1131−1151.

(2) Van Bambeke, F., Harms, J. M., Van Laethem, Y., and Tulkens, P. M. (2008) Ketolides: Pharmacological profile and rational positioning in the treatment of respiratory tract infections. *Expert Opin. Pharmacother. 9*, 267−283.

(3) Rafie, S., MacDougall, C., and James, C. L. (2010) Cethromycin: A promising new ketolide antibiotic for respiratory infections. *Pharmacotherapy 30*, 290−303.

(4) Pletz, M. W., Welte, T., and Ott, S. R. (2010) Advances in the prevention, management, and treatment of community-acquired pneumonia. *F1000 Med. Rep. 2*, 53.

(5) Carratala, J., and Garcia-Vidal, C. (2010) An update on Legionella. *Curr. Opin. Infect. Dis. 23*, 152−157.

(6) Hammerschlag, M. R., and Sharma, R. (2008) Use of cethromycin, a new ketolide, for treatment of community-acquired respiratory infections. *Expert Opin. Invest. Drugs 17*, 387−400.

(7) Palusinska-Szysz, M., and Cendrowska-Pinkosz, M. (2009) Pathogenicity of the family Legionellaceae. *Arch. Immunol. Ther. Exp. 57*, 279−290.

(8) Poehlsgaard, J., and Douthwaite, S. (2005) The bacterial ribosome as a target for antibiotics. *Nat. Rev. Microbiol. 3*, 870−881.

(9) Kirst, H. A. (2010) New macrolide, lincosaminide and streptogramin B antibiotics. *Expert Opin. Ther. Pat. 20*, 1343−1357.

(10) Devasahayam, G., Scheld, W. M., and Hoffman, P. S. (2010) Newer antibacterial drugs for a new century. *Expert Opin. Invest. Drugs 19*, 215−234.

(11) Nakajima, Y. (1999) Mechanisms of bacterial resistance to macrolide antibiotics. *J. Infect. Chemother. 5*, 61−74.

(12) Weisblum, B. (1998) Macrolide resistance. *Drug Resist. Updates 1*, 29−41.

(13) Ounissi, H., and Courvalin, P. (1985) Nucleotide sequence of the gene ereA encoding the erythromycin esterase in *Escherichia coli*. *Gene 35*, 271−278.

(14) Arthur, M., Autissier, D., and Courvalin, P. (1986) Analysis of the nucleotide sequence of the ereB gene encoding the erythromycin esterase type II. *Nucleic Acids Res. 14*, 4987−4999.

(15) Arthur, M., Andremont, A., and Courvalin, P. (1987) Distribution of erythromycin esterase and rRNA methylase genes in members of the family Enterobacteriaceae highly resistant to erythromycin. *Antimicrob. Agents Chemother. 31*, 404−409.

(16) Nakamura, A., Nakazawa, K., Miyakozawa, I., Mizukoshi, S., Tsurubuchi, K., Nakagawa, M., O'Hara, K., and Sawai, T. (2000) Macrolide esterase-producing *Escherichia coli* clinically isolated in Japan. *J. Antibiot. 53*, 516−524.

(17) Peters, E. D., Leverstein-van Hall, M. A., Box, A. T., Verhoef, J., and Fluit, A. C. (2001) Novel gene cassettes and integrons. *Antimicrob. Agents Chemother. 45*, 2961−2964.

(18) Yong, D., Toleman, M. A., Giske, C. G., Cho, H. S., Sundman, K., Lee, K., and Walsh, T. R. (2009) Characterization of a new metallo-β-lactamase gene, bla(NDM-1), and a novel erythromycin esterase gene carried on a unique genetic structure in *Klebsiella pneumoniae* sequence type 14 from India. *Antimicrob. Agents Chemother. 53*, 5046−5054.

(19) Murphy, B. P., O'Mahony, R., Buckley, J. F., Shine, P., Boyd, E. F., Gilroy, D., and Fanning, S. (2007) Investigation of a global collection of nontyphoidal *Salmonella* of various serotypes cultured between 1953 and 2004 for the presence of class 1 integrons. *FEMS Microbiol. Lett. 266*, 170−176.

(20) Krauland, M., Harrison, L., Paterson, D., and Marsh, J. (2010) Novel integron gene cassette arrays identified in a global collection of multi-drug resistant non-typhoidal *Salmonella enterica*. *Curr. Microbiol. 60*, 217−223.

(21) Thungapathra, M., Amita, Sinha, K. K., Chaudhuri, S. R., Garg, P., Ramamurthy, T., Nair, G. B., and Ghosh, A. (2002) Occurrence of antibiotic resistance gene cassettes aac(6′)-Ib, dfrA5, dfrA12, and ereA2 in class I integrons in non-O1, non-O139 *Vibrio cholerae* strains in India. *Antimicrob. Agents Chemother. 46*, 2948−2955.

(22) Biskri, L., and Mazel, D. (2003) Erythromycin esterase gene ere(A) is located in a functional gene cassette in an unusual class 2 integron. *Antimicrob. Agents Chemother. 47*, 3326−3331.

(23) Arthur, M., Brisson-Noel, A., and Courvalin, P. (1987) Origin and evolution of genes specifying resistance to macrolide, lincosamide and streptogramin antibiotics: Data and hypotheses. *J. Antimicrob. Chemother. 20*, 783−802.

(24) O'Hara, K., and Yamamoto, K. (1996) Reaction of roxithromycin and clarithromycin with macrolide-inactivating enzymes from highly erythromycin-resistant *Escherichia coli*. *Antimicrob. Agents Chemother. 40*, 1036−1038.

(25) Barthelemy, P., Autissier, D., Gerbaud, G., and Courvalin, P. (1984) Enzymic hydrolysis of erythromycin by a strain of *Escherichia coli*. A new mechanism of resistance. *J. Antibiot. 37*, 1692−1696.

(26) Kim, Y. H., Cha, C. J., and Cerniglia, C. E. (2002) Purification and characterization of an erythromycin esterase from an erythromycin-resistant *Pseudomonas* sp. *FEMS Microbiol. Lett. 210*, 239−244.

(27) Gerlt, J. A., and Babbitt, P. C. (2001) Divergent evolution of enzymatic function: Mechanistically diverse superfamilies and functionally distinct suprafamilies. *Annu. Rev. Biochem. 70*, 209−246.

(28) Morar, M., and Wright, G. D. (2010) The genomic enzymology of antibiotic resistance. *Annu. Rev. Genet. 44*, 25−51.

(29) Bauer, A. W., Kirby, W. M., Sherris, J. C., and Turck, M. (1966) Antibiotic susceptibility testing by a standardized single disk method. *Am. J. Clin. Pathol. 45*, 493−496.

(30) McGuffin, L. J., Bryson, K., and Jones, D. T. (2000) The PSIPRED protein structure prediction server. *Bioinformatics 16*, 404−405.

(31) Eswar, N., Webb, B., Marti-Renom, M. A., Madhusudhan, M. S., Eramian, D., Shen, M. Y., Pieper, U., and Sali, A. (2006) Comparative protein structure modeling using Modeller. *Current Protocols in Bioinformatics*, Chapter 5, Unit 5, p 6, Wiley, New York.

(32) Fett, W. F., Gerard, H. C., Moreau, R. A., Osman, S. F., and Jones, L. E. (1992) Screening of nonfilamentous bacteria for production of cutin-degrading enzymes. *Appl. Environ. Microbiol. 58*, 2123−2130.

(33) Marchler-Bauer, A., Lu, S., Anderson, J. B., Chitsaz, F., Derbyshire, M. K., DeWeese-Scott, C., Fong, J. H., Geer, L. Y., Geer, R. C., Gonzales, N. R., Gwadz, M., Hurwitz, D. I., Jackson, J. D., Ke, Z., Lanczycki, C. J., Lu, F., Marchler, G. H., Mullokandov, M., Omelchenko, M. V., Robertson, C. L., Song, J. S., Thanki, N., Yamashita, R. A., Zhang, D., Zhang, N., Zheng, C., and Bryant, S. H. (2010) CDD: A Conserved Domain Database for the functional annotation of proteins. *Nucleic Acids Res. 39*, D225−D229.

(34) Edgar, R. C. (2004) MUSCLE: Multiple sequence alignment with high accuracy and high throughput. *Nucleic Acids Res. 32*, 1792−1797.

(35) Engel, P. C. (1977) *Enzyme Kinetics: The Steady-State Approach*, Wiley, New York.

(36) Nelson, D. L., and Cox, M. M. (2000) *Lehninger Principles of Biochemistry*, New York, W. H. Freeman.

(37) Harel, M., Aharoni, A., Gaidukov, L., Brumshtein, B., Khersonsky, O., Meged, R., Dvir, H., Ravelli, R. B., McCarthy, A., Toker, L., Silman, I., Sussman, J. L., and Tawfik, D. S. (2004) Structure and evolution of the serum paraoxonase family of detoxifying and anti-atherosclerotic enzymes. *Nat. Struct. Mol. Biol. 11*, 412−419.

(38) Afriat, L., Roodveldt, C., Manco, G., and Tawfik, D. S. (2006) The latent promiscuity of newly identified microbial lactonases is linked to a recently diverged phosphotriesterase. *Biochemistry 45*, 13677−13686.

(39) Draganov, D. I. (2010) Lactonases with organophosphatase activity: Structural and evolutionary perspectives. *Chem.-Biol. Interact. 187*, 370−372.

(40) Liu, D., Lepore, B. W., Petsko, G. A., Thomas, P. W., Stone, E. M., Fast, W., and Ringe, D. (2005) Three-dimensional structure of the quorum-quenching N-acyl homoserine lactone hydrolase from *Bacillus thuringiensis*. *Proc. Natl. Acad. Sci. U.S.A. 102*, 11882−11887.

(41) Testa, B., and Mayer, J. M. (2003) *Hydrolysis in drug and prodrug metabolism*, Verlag Helvetica Chimica Acta, Wiley-VCH, Berlin.
(42) Testa, B., and Kramer, S. D. (2007) The biochemistry of drug metabolism—an introduction: Part 2. Redox reactions and their enzymes. *Chem. Biodiversity 4*, 257−405.
(43) Holm, L., and Rosenstrom, P. (2010) Dali server: Conservation mapping in 3D. *Nucleic Acids Res. 38*, W545−W549.
(44) Chan, A. C., Lelj-Garolla, B., I Rosell, F., Pedersen, K. A., Mauk, A. G., and Murphy, M. E. (2006) Cofacial heme binding is linked to dimerization by a bacterial heme transport protein. *J. Mol. Biol. 362*, 1108−1119.
(45) Anantharaman, V., Aravind, L., and Koonin, E. V. (2003) Emergence of diverse biochemical activities in evolutionarily conserved structural scaffolds of proteins. *Curr. Opin. Chem. Biol. 7*, 12−20.
(46) Brennan, T. V., Anderson, J. W., Jia, Z., Waygood, E. B., and Clarke, S. (1994) Repair of spontaneously deamidated HPr phosphocarrier protein catalyzed by the L-isoaspartate-(D-aspartate) O-methyltransferase. *J. Biol. Chem. 269*, 24586−24595.
(47) Griffith, S. C., Sawaya, M. R., Boutz, D. R., Thapar, N., Katz, J. E., Clarke, S., and Yeates, T. O. (2001) Crystal structure of a protein repair methyltransferase from *Pyrococcus furiosus* with its L-isoaspartyl peptide substrate. *J. Mol. Biol. 313*, 1103−1116.
(48) Furuchi, T., Sakurako, K., Katane, M., Sekine, M., and Homma, H. (2010) The role of protein L-isoaspartyl/D-aspartyl O-methyltransferase (PIMT) in intracellular signal transduction. *Chem. Biodiversity 7*, 1337−1348.
(49) Smith, C. D., Carson, M., Friedman, A. M., Skinner, M. M., Delucas, L., Chantalat, L., Weise, L., Shirasawa, T., and Chattopadhyay, D. (2002) Crystal structure of human L-isoaspartyl-O-methyl-transferase with S-adenosyl homocysteine at 1.6-Å resolution and modeling of an isoaspartyl-containing peptide at the active site. *Protein Sci. 11*, 625−635.